APPLIED AND ENVIRONMENTAL MICROBIOLOGY, Jan. 2005, p. 371–381 Vol. 71, No. 1
0099-2240/05/$08.00+0 doi:10.1128/AEM.71.1.371–381.2005

Role of Oxalic Acid Overexcretion in Transformations of Toxic Metal Minerals by *Beauveria caledonica*

M. Fomina,[1] S. Hillier,[2] J. M. Charnock,[3] K. Melville,[1] I. J. Alexander,[4] and G. M. Gadd[1]*

Division of Environmental and Applied Biology, Biological Sciences Institute, School of Life Sciences, University of Dundee, Dundee,[1] Macaulay Land Use Research Institute, Craigiebuckler,[2] and Department of Plant and Soil Science, University of Aberdeen, Aberdeen,[4] Scotland, and Synchrotron Radiation Source Daresbury Laboratory, Daresbury, Warrington, Cheshire,[3] United Kingdom

Received 9 June 2004/Accepted 29 August 2004

The fungus *Beauveria caledonica* was highly tolerant to toxic metals and solubilized cadmium, copper, lead, and zinc minerals, converting them into oxalates. This fungus was found to overexcrete organic acids with strong metal-chelating properties (oxalic and citric acids), suggesting that a ligand-promoted mechanism was the main mechanism of mineral dissolution. Our data also suggested that oxalic acid was the main mineral-transforming agent. Cadmium, copper, and zinc oxalates were precipitated by the fungus in the local environment and also in association with the mycelium. The presence of toxic metal minerals often led to the formation of mycelial cords, and in the presence of copper-containing minerals, these cords exhibited enhanced excretion of oxalic acid, which resulted in considerable encrustation of the cords by copper oxalate hydrate (moolooite). It was found that *B. caledonica* hyphae and cords were covered by a thick hydrated mucilaginous sheath which provided a microenvironment for chemical reactions, crystal deposition, and growth. Cryo-scanning electron microscopy revealed that mycogenic metal oxalates overgrew parental fungal hyphae, leaving a labyrinth of fungal tunnels within the newly formed mineral matter. X-ray absorption spectroscopy revealed that oxygen ligands played a major role in metal coordination within the fungal biomass during the accumulation of mobilized toxic metals by *B. caledonica* mycelium; these ligands were carboxylic groups in copper phosphate-containing medium and phosphate groups in pyromorphite-containing medium.

Fungi, which are a major and often dominant component of the microbiota in soils and mineral substrates, are important as decomposer organisms, animal and plant symbionts and pathogens, and spoilage organisms of natural and synthetic materials, and they play an important role in biogeochemical cycles of elements (7, 17, 18). Certain fungal processes solubilize metals from minerals and bound locations, thereby increasing metal bioavailability, whereas other fungal processes immobilize metals and reduce their bioavailability (7, 18). Flexible mycelial growth strategies and the ability to produce and exude organic acids, protons, and other metabolites make fungi important biological weathering agents of natural rock, minerals, and building materials (7, 16, 18). As mineral components contain considerable quantities of metals, as well as other elements which are biologically unavailable, the influence of such processes on metal mobility are of economic and environmental significance and may be important in the treatment or natural attenuation of contaminated soil (17).

Metal mobilization by fungi can occur as a result of several mechanisms, including acidolysis (proton promoted), complexolysis (ligand promoted), reductive mobilization, and the mycelium functioning as a sink for soluble metal species (8). These processes include proton efflux and the production of siderophores [for Fe(III)], but in many strains leaching occurs due to the production of primary and secondary metabolites with metal-chelating properties (e.g., carboxylic acids, amino acids, and phenolic compounds); thus, there are both proton- and ligand-mediated mechanisms of mobilization that play an integral role in chemical attack of mineral surfaces (7, 8, 19, 36, 39).

Most previous studies have focused on the dissolution and transformation of calcium-containing minerals (calcium phosphates, carbonate, and sulfate) by fungi (7, 33, 49). Free-living saprotrophic soil fungi and ericoid and ectomycorrhizal fungi have also been studied for their abilities to dissolve toxic metal-bearing minerals (34, 37, 42, 43, 44). However, potentially entomopathogenic fungi, such as *Beauveria* species, have been neglected, and there is no information on the mineral-solubilizing and -transforming potential of this group of fungi. This is hardly surprising as most research has concentrated on the relationship of the fungus with an insect host and its pathogenicity for the host and on implications for plant protection and biological control. However, there is now compelling evidence that this group of fungi is able to exploit almost all ecophysiological niches and can exhibit a capacity for saprotrophy, necrotrophy, and biotrophy. *Beauveria caledonica*, which was first isolated from Scottish moorland soil, was found to be saprotrophically active and a significant biological competitor in soil (3). It is now known that *Beauveria* species not only are able to infect a wide range of insects and grow as soil saprophytes but also can survive as plant endophytes. The latter phenomenon supports the bodyguard hypothesis that proposes that plants may gain advantages from the presence of other organisms, such as fungi, that provide a defense against herbivores (5, 15, 48, 51). Fungi similar to entomopathogenic species (*Verticillium* sp.) were some of the main components of

* Corresponding author. Mailing address: Division of Environmental and Applied Biology, Biological Sciences Institute, School of Life Sciences, University of Dundee, Dundee DD1 4HN, Scotland, United Kingdom. Phone: 44 1382 344765. Fax: 44 1382 348216. E-mail: g.m.gadd@dundee.ac.uk.

Antarctic microbial endolithic communities within the gypsum crust (27). It can be suggested that this group of fungi may colonize successfully any econiche where insects can exist, such as soil, plants, mushrooms, rocks, minerals, and building materials. Their unique ability to exploit a wide range of habitats, as well as their biochemical potential, may therefore underpin a more significant role in geochemical changes in the terrestrial environment than has hitherto been appreciated.

The aim of this work was therefore to examine the ability of the entomopathogenic fungus *B. caledonica* to tolerate, solubilize, and transform toxic metal minerals, as well as the physicochemical mechanisms involved in such transformations and metal accumulation by the biomass.

MATERIALS AND METHODS

Organism, origin, and identification. The fungal strain used was isolated from lawn soil (United Kingdom) and was provided by D. Genney (CEH Merlewood collection). In a preliminary screening of several fungal soil isolates for the ability to dissolve and transform toxic metal minerals, this isolate exhibited a unique potential compared to other strains, and so in further studies we focused on its identification and mineral transformation ability.

DNA extraction, purification, PCR, and sequencing. Mycelium was scraped into a 2.5-ml bead beating tube with 1 ml of a buffer solution comprising sodium dodecyl sulfate (5%, wt/vol), Tris (50 mM), NaCl (50 mM), and EDTA (10 mM) (pH 8.0). Cells were disrupted by using a mini-bead beater (Biospec Products, Inc., Bartlesville, Okla.) for 45 s. Following bead beating, the tubes were centrifuged at 14,000 × *g* for 5 min, and the DNA in the supernatant was extracted with phenol-chloroform. The DNA was then ethanol precipitated and further purified by using a Roche PCR clean-up kit (Roche Diagnostics GmbH, Mannheim, Germany) according to the manufacturer's instructions. Extractions were performed in duplicate with negative controls.

The eukaryotic internal transcribed spacer region was amplified by using primers ITS1F and ITS4, and the expected product size was approximately 650 bp (52). PCRs were performed in duplicate with controls in 50-μl mixtures containing 5 μl of 10× PCR buffer, 3 mM $MgCl_2$, each deoxynucleoside triphosphate at a concentration of 200 μM, 1.25 U of *Taq* polymerase (QIAGEN GmbH, Hilden, Germany), each primer (Invitrogen Life Technologies, Paisley, United Kingdom) at a concentration of 1 μM, 25 mg of bovine serum albumin ml^{-1}, and ~20 ng of template DNA. The cycling parameters were as follows: initial denaturation at 94°C for 1 min 25 s, followed by 35 cycles of 95°C for 35 s, 52°C for 55 s, and 72°C for 1 min and then a final elongation step of 72°C for 10 min. Amplified DNA fragments were visualized by ethidium bromide staining on 1% agarose gels.

PCR products were further purified with the Roche PCR clean-up kit (Roche Diagnostics GmbH). Duplicate purified PCR products were then sequenced by using Applied Biosystems Big-Dye chemistry with an Applied Biosystems model 3100 automated capillary DNA sequencer (DNA Analysis Facility, Department of Molecular and Cellular Pathology, Ninewells Hospital, University of Dundee, Dundee, Scotland) (http://www.humangenetics.org.uk/dnaseq.htm). Approximately 550 bp of sequence information was obtained for the internal transcribed spacer region of each duplicate fungal isolate. The identity was determined by comparing the sequence data with the GenBank database. The sequence of the isolate exhibited the highest level of homology (99%) with *B. caledonica* (accession number U19043).

Media and culture conditions. The organism was maintained at 25°C on modified Melin-Norkrans agar medium, which contained (per liter) 0.5 g of $(NH_4)_2HPO_4$, 0.3 g of KH_2PO_4, 0.14 g of $MgSO_4 \cdot 7H_2O$, 0.05 g of $CaCl_2 \cdot 6H_2O$, 0.025 g of NaCl, 10 g of D-glucose, 0.001 g of glutamic acid, 0.0001 g of thiamine, and 14 g of agar no. 1 (Lab M, Bury, United Kingdom). Before the agar was added and before autoclaving, the pH of the liquid medium was adjusted to 5.5 with 1 M HCl. All mineral solubilization experiments were carried out by using modified Melin-Norkrans agar supplemented with the appropriate metal compounds at the desired final concentrations. The metal compounds were oven sterilized for 36 to 48 h at 95°C.

Metal compounds. Commercial preparations of $Cd_3(PO_4)_2$ (Alfa), $Cu_3(PO_4)_2 \cdot 2H_2O$ (Fluka), Cu_2O (BDH, Poole, United Kingdom) (naturally occurring as cuprite), $Zn_3(PO_4)_2 \cdot 2H_2O$ (Alfa) (naturally occurring as hopeite), $Pb_3(PO_4)_2$ (Alfa), $PbCO_3$ (BDH) (naturally occurring as cerussite), Pb_3O_4 (Aldrich) (red lead), and PbS (Aldrich) (naturally occurring as galena) were used. Lead chlorophosphate or pyromorphite [$Pb_5(PO_4)_3Cl$] was synthesized by mixing solutions of Pb, P, and Cl in stoichiometric proportions (5:3:1); 200 ml of 0.5 M $Pb(NO_3)_2$ was mixed with 200 ml of a solution containing 0.3 M Na_2HPO_4 and 0.1 M NaCl at approximately 90°C. When it was cool, the precipitate was separated by filtration, washed with deionized water, and dried at 60°C (44). Samples of the pyromorphite obtained were examined by using X-ray powder diffraction (XRPD) to confirm their homogeneity.

Growth and mineral solubilization. (i) Preparation of metal-amended plates and inoculation. The fungus was grown on 20 cm^3 of modified Melin-Norkrans agar in 90-mm-diameter petri dishes with metal compounds added to a final metal concentration equivalent to 15 mM (42, 43). Metal phosphates and Pb_3O_4 were added to a final concentration of 5 mM. Cu_2O was added to a final concentration of 7.5 mM, PbS and $PbCO_3$ were added to a final concentration of 15 mM, and $Pb_5(PO_4)_3Cl$ was added to a final concentration of 3 mM in order to equalize metal concentrations in molar terms. Prior to inoculation, 84-mm-diameter disks of sterile cellophane membrane were placed aseptically on the surface of the agar in each petri dish (43). Inoculation was carried out by using 7-mm-diameter disks of mycelium cut from the leading edge of colonies which had been maintained on modified Melin-Norkrans agar at 25°C for at least 14 days. The fungus was inoculated onto each metal compound (at least three replicates) and incubated at 25°C for 2 months. The sizes of the colonies and of any clear zones present were measured every 3 to 4 days.

(ii) Abiotic test. The ability of commercial oxalic acid (BDH) to solubilize $Zn_3(PO_4)_2$, $Cd_3(PO_4)_2$, $Cu_3(PO_4)_2$, and $Pb_5(PO_4)_3Cl$ was also tested. The tests were carried out by using the same petri dish microcosms with 20 cm^3 of modified Melin-Norkrans agar with metal compounds added to final metal concentrations equivalent to 15 mM. Cadmium, copper, and zinc phosphates were added to a final concentration of 5 mM, and $Pb_5(PO_4)_3Cl$ was added to a final concentration 3 mM. Oxalic acid (0.1 ml) was added at concentrations up to 1 M to wells bored in the agar (diameter, 7 mm).

(iii) Estimation of solubilizing ability. The main criterion used for mineral-solubilizing ability was the diameter of the solubilization area (clear halo) in the agar underneath and/or around a colony used previously in studies of fungal phosphate-solubilizing ability and mineral transformation (42, 43).

(iv) Biomass and metal analysis. Colonies were removed from replicate agar plates by peeling the biomass from the dialysis membrane. The mycelia were oven dried at 80°C until a constant weight was reached and, after the dry weight was measured, were digested (0.05 g) in 3.0 ml of concentrated HNO_3 at 115°C overnight in a digestion block (Grant Instruments, Shepreth, United Kingdom). After appropriate dilution with double-distilled H_2O, the metal ion contents of the solutions were analyzed by using a Pye Unicam SP9 atomic absorption spectrophotometer with comparisons to appropriate standard solutions in acidified double-distilled H_2O.

(v) Metal tolerance. Growth of the fungus was evaluated by determining the extension of a colony and the dry weight since the extension of a colony alone does not take into account the density of the fungal mycelium (11). The tolerance results were expressed as a tolerance index (TI) based on the dry weights of fungal biomass, as follows: TI = (dry weight of treated mycelium/dry weight of control mycelium) × 100%.

Organic acid analysis. For analysis of organic acid excretion, the organism was grown in a liquid static culture in 12 cm^3 of modified Melin-Norkrans medium (as described above, without agar) in sterile plastic flat flasks with a total volume 50 ml and a growth area 25 cm^2 (CellStar tissue culture flasks; Greiner Bio-One, Kremsmunster, Austria). Static cultures were used rather than submerged shake cultures because (i) this method better simulated the environmental conditions for fungal biogeochemical activity in nature and (ii) this method gave better results for metal transformation due to the preservation of undisturbed fungal mycelium and its microenvironment in which the mineral solubilization and transformation processes occurred. Cu_2O was added to a final concentration of 7.5 mM, $Pb_5(PO_4)_3Cl$ was added to a final concentration of 3 mM, and $Zn_3(PO_4)_2$ and Pb_3O_4 were added to a final concentration of 5 mM. Inoculation was carried out with 7-mm-diameter disks of mycelium cut from the leading edges of colonies which had been maintained on modified Melin-Norkrans agar at 25°C for at least 14 days. The fungus was incubated at 25°C for 60 days, and at least three replicates were used. Growth, mineral solubilization, and transformation were observed macro- and microscopically.

Metal phosphates and Pb_3O_4 were added to a final concentration of 5 mM. Cu_2O was added to a final concentration of 7.5 mM, PbS and $PbCO_3$ were added to a final concentration of 15 mM, and $Pb_5(PO_4)_3Cl$ was added to a final concentration of 3 mM in order to equalize metal concentrations in molar terms.

During fungal growth, aliquots (1 ml) of the liquid cultures were removed and used for analysis of organic acid (carboxylic acid) production. The analysis was carried out using a high-performance liquid chromatography system comprising

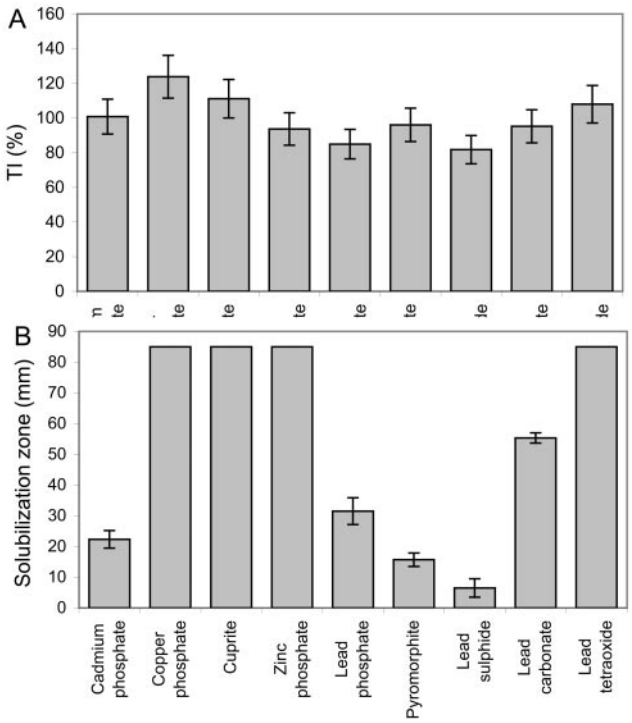

FIG. 1. Ability of *B. caledonica* to tolerate and dissolve toxic metal minerals. (A) Tolerance indices (TI) calculated from the biomass yields on mineral-containing and mineral-free agar media (dry weight of treated mycelium/dry weight of control mycelium × 100%). (B) Solubilization of minerals in agar media expressed as solubilization zone diameters. The values are means derived from at least four replicate determinations. The error bars indicate standard errors of the means; where error bars are not shown, they were less than the graph dimensions.

a Waters (Watford, Herts, United Kingdom) 600E system controller, a Waters 490E programmable multiwavelength detector, a Waters U6K pump, and a Waters 7171 plus autosampler controlled by Millipore (Waters) Millennium chromatography software. Sulfuric acid (8 mM; Aristar, BDH) was used to elute fractions from an Aminex HPX-87H high-performance liquid chromatography organic acid analysis ion-exclusion column (Bio-Rad, Richmond, Calif.). To remove free metal species, samples were treated with ion-exchange resin (AG 50W-X8 100–200 hydrogen form resin; Bio-Rad). Both samples and eluant were prefiltered through 0.45-μm-pore-size membrane filters (cellulose acetate; 13-mm-diameter syringe filter; Alltech Associates Ltd., Carnforth, United Kingdom), and then 20-μl portions of triplicate samples were eluted for 30 min. Oxalic acid production was also analyzed enzymatically by using a commercial kit (Sigma Diagnostics catalog no. 591-D; Sigma-Aldrich Company Ltd., Poole, Dorset, United Kingdom).

Statistical analysis. Minitab for Windows 12 (release 12.1) was used for statistical analysis. At least three replicate determinations were used in experiments.

Analysis of mineral transformation products. Following light microscopic observations, scanning electron microscopy (SEM)-based techniques, including environmental SEM (ESEM) and cryo-SEM, were used to analyze metal-mineral transformations.

(i) ESEM high-vacuum mode. Conventional SEM has been successfully used to study metal oxalates precipitated by fungi (43). However, the precipitation of secondary mycogenic minerals on the surfaces of fungal hyphae is less well understood due to the loss of mineral precipitates during conventional preparation techniques. We used air drying to study crystal formation on hyphae during their growth on medium amended with insoluble minerals. The samples were then coated with 30 nm of Au-Pd by using a Cressington 208 HR sputter coater and were examined with a Philips XL30 environmental scanning electron microscope field emission gun operating at an accelerating voltage of 15 or 25 kV.

(ii) ESEM wet mode. A Philips XL30 environmental scanning electron microscope field emission gun was used to study fully hydrated samples in their natural environment. The main environmental SEM capabilities relevant to our study were (i) secondary electron imaging in gas or water vapor at a full SEM resolution of at least 2 nm; (ii) imaging of wet samples with no dehydration; (iii) observation of the sample in its natural environment; (iv) no sample preparation required; and (v) X-ray analysis of nonconductive samples.

(iii) Cryo-SEM. Cryo-preparation of fungal specimens is one of the best ways to preserve fragile mycelium for SEM study and allows observation of both interior and exterior structures of cryo-fractured samples. A specimen was held in the jaws of a sample holder, and Tissue-Tek, which acts as a glue when it is frozen, was smeared around the base of the sample. Liquid N_2 was placed under a vacuum in the freezing chamber (Alto2500) until it became solid (slush). The chamber was then brought back to atmospheric pressure, and the sample was immediately plunged into the chamber and a vacuum was reapplied. The sample was withdrawn from the chamber just before the N_2 resolidified. The sample was then transferred under a vacuum to the preparation chamber. After fracturing, the sample was warmed to −95°C for 5 min to remove the surface water. After sublimation, the sample was cooled to −115°C prior to coating with approximately 5 nm of Au-Pd. Samples were examined by using an Hitachi S-4700 field emission gun scanning electron microscope operating at an accelerating voltage of 5 kV.

(iv) EDXA. Mineral precipitates in the media and in mycelia were analyzed by using energy-dispersive X-ray analysis (EDXA) and a Philips XL30 environmental scanning electron microscope field emission gun.

(v) XRPD analysis. All the products of mineral transformation by the fungus in the media and in mycelia were analyzed by X-ray powder diffraction (XRPD). The samples were sprinkled onto low-background silicon crystal holders and scanned from 2 to 75° 2Ø with a Siemens D5000 diffractometer by using cobalt Kα radiation selected with a diffracted beam monochromator. Each sample was counted for 1 s per step by using a step size of 0.02°. The slits used were 1° divergence, 1° antiscatter, and a 0.6-mm receiving slit. The broad peak centered at around 7Å was diffraction from the plastic sample holder surround. Phases were identified by reference to patterns in the powder diffraction file.

(vi) Copper oxalate hydrate solubility. Mycogenic copper oxalate hydrate crystals were soluble in NH_4OH but not in acetic acid, HCl, or HNO_3, which allowed us to calculate the ratio of the moolooite crystals precipitated on the mycelium to the total copper accumulated by fungal biomass.

X-ray absorption spectroscopy of fungal biomass. (i) Copper. X-ray absorption spectra at the Cu K-edge were collected at Station 7.1 at the CLRC Daresbury Synchrotron Radiation Source operating at 2 GeV with an average current of 140 mA by using a vertically collimating plane mirror and a sagitally bent focusing Si(111) double crystal monochromator detuned to 80% transmission to minimize harmonic contamination. Sample data were collected with the station operating in the fluorescence mode by using a nine-element solid-state Ge diode detector with high-count-rate XPRESS processing electronics; spectra of model compounds were collected in the transmission mode. The monochromator was calibrated by using a 5-μg Cu foil. Experiments were performed by using a liquid nitrogen-cooled cryostat. Single scans were collected for the model compounds, and three or four scans were collected and summed for each sample.

(ii) Lead. X-ray absorption spectra at the Pb L(III)-edge were collected at Station 16.5 at the CLRC Daresbury Synchrotron Radiation Source operating at 2 GeV with an average current of 150 mA by using a vertically focusing mirror and a sagitally bent focusing Si(220) double crystal monochromator detuned to 70% transmission to minimize harmonic rejection. Data were collected with the station operating in the fluorescence mode by using an Ortec 30 element solid-state Ge detector. The monochromator calibration was checked by using a $Pb_3(PO_4)_2$ standard. Experiments were performed in a liquid nitrogen-cooled cryostat. Spectra of model compounds were collected in the transmission mode. Single scans were collected for the model compounds, and three or four scans were collected and summed for each sample.

(iii) EXAFS spectrum analysis. Background-subtracted extended X-ray absorption fine-structure (EXAFS) spectra were analyzed in EXCURV98 by using full curved wave theory (1, 22). Phase shifts were derived in the program from ab initio calculations by using Hedin-Lundqvist potentials and von Barth ground states (25). Fourier transforms of the EXAFS spectra were used to obtain an approximate radial distribution function around the central atom (the absorber atom); the peaks of the Fourier transform could be related to shells of surrounding back scattering atoms characterized by atom type, number of atoms in the shell, the absorber-scatterer distance, and the Debye-Waller factor, $2\sigma^2$ (a measure of both the thermal motion between the absorber and the scatterer and the static disorder or range of absorber-scatterer distances). The data were fitted for

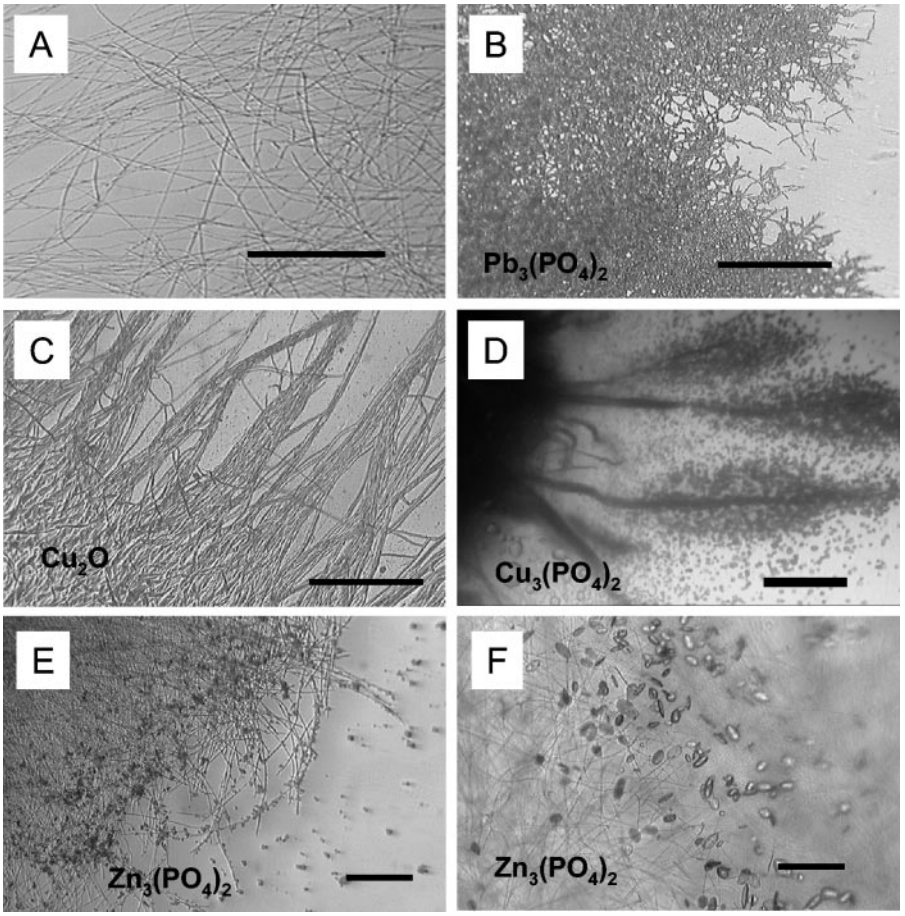

FIG. 2. (A to D) Morphological responses of marginal zones of *B. caledonica* colonies to toxic metal minerals after 3 weeks of growth at 25°C. (A) Loose control mycelium on mineral-free medium; (B and C) dense mycelium grown on media containing lead phosphate (B) and cuprite (C); (D) hyphal cords encrusted by copper oxalate hydrate crystals on medium containing copper phosphate. (A to C) Scale bars = 50 μm; (D) scale bar = 1,000 μm. (E and F) Light microscopic images of the transformation of zinc phosphate into zinc oxalate dihydrate by *B. caledonica* in liquid static culture. (E) Zinc phosphate particles adsorbed by the fungal mycelium after 7 days of growth at 25°C; (F) crystals of zinc oxalate dihydrate in the same mycelium after 10 days of growth at 25°C. Scale bars = 20 μm.

each sample by defining a theoretical model and comparing the calculated EXAFS spectrum with the experimental data. Shells of backscatterers were added around the central atom, and by refining an energy correction E_f (the Fermi energy), the absorber-scatterer distance, and the Debye-Waller factor for each shell, a least-squares residual (the R factor [2]) was minimized. Where appropriate, multiple scattering effects were included in the fits (23).

RESULTS

B. caledonica was highly tolerant to all toxic metal-containing minerals tested, and the tolerance index values were all around 100% (Fig. 1A). However, the morphological patterns of the marginal zones of the colonies were significantly altered by the presence of toxic metal minerals in solid medium (Fig. 2). In general, toxic metal minerals (e.g., lead phosphate and cuprite) induced mycelial aggregation or the so-called phalanx growth strategy and resulted in a very dense mycelium compared to the control growth pattern (Fig. 2A to C). The presence of copper phosphate in the medium resulted in atypical formation of mycelial cords (aggregations of longitudinally aligned hyphae) (Fig. 2D).

According to the data for mineral solubilization in agar and microscopic examination of changes in the metal-containing minerals, *B. caledonica* was able to solubilize all of the insoluble minerals tested to some degree (Fig. 1B). Copper phosphate, cuprite, zinc phosphate, and lead tetraoxide were fully solubilized in whole-petri-dish microcosms, and portions of the minerals were transformed into secondary mycogenic precipitates. The order for the ability to solubilize the other minerals was as follows: lead carbonate > lead phosphate > cadmium phosphate > pyromorphite > lead sulfide (Fig. 1B).

Complementary experiments with liquid media containing zinc phosphate, cuprite, and lead tetraoxide revealed that *B. caledonica* produced considerable amounts of organic acids (Fig. 3). In all cases, including the control, the fungus excreted millimolar amounts (0.6 to 2 mM) of oxalic acid during growth in static liquid culture. The presence of toxic metal-containing minerals led to the formation of citric acid after 10 to 20 days of growth and, in the case of zinc phosphate, acetate during the first 10 days of growth (Fig. 3) and malic acid (0.1 mM) (data not shown). On the 20th day of growth, the citric acid concentration reached 7 and 13 mM with zinc phosphate and cuprite, respectively (Fig. 3). Between the 7th and 10th days of static

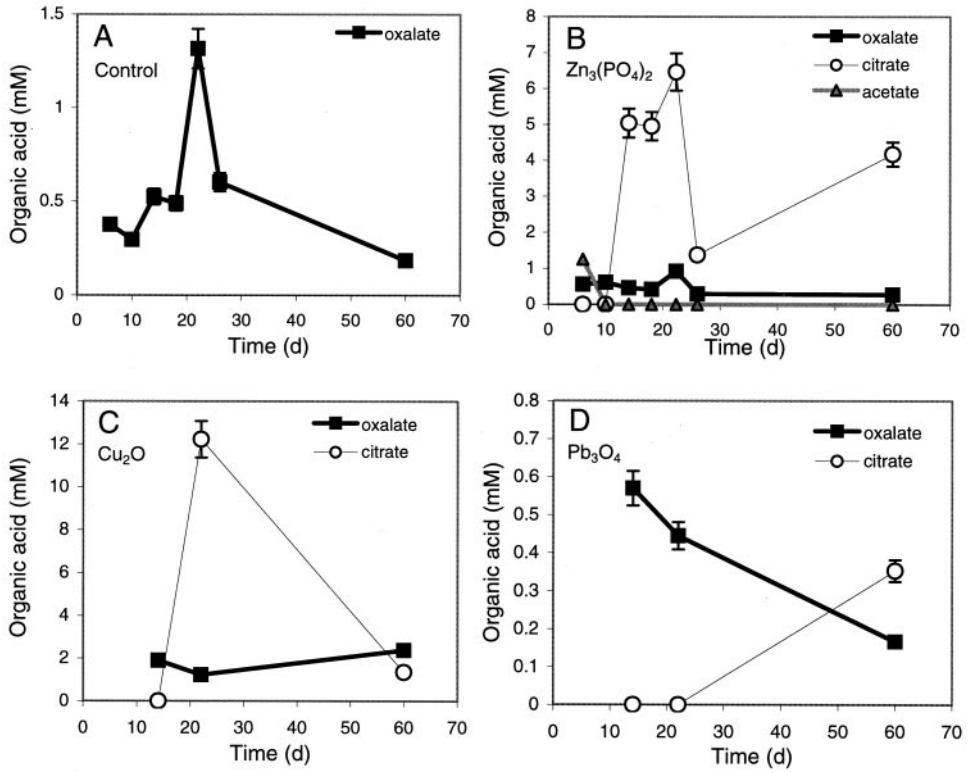

FIG. 3. Organic acid production by *B. caledonica* in liquid static cultures on mineral-free control medium (A) and media containing zinc phosphate (B), cuprite (C), and lead tetraoxide (D). The values are means derived from at least three replicate determinations. The error bars indicate standard errors of the means; where error bars are not shown, they were less than the dimensions of the symbols.

growth, *B. caledonica* transformed zinc phosphate particles adsorbed to the mycelium into zinc oxalate dihydrate crystals, and the level of oxalate excreted remained approximately 0.6 mM (Fig. 2E and F and 3).

The presence of solubilization zones in abiotic (fungus-free) agar systems in petri dishes containing cadmium, copper, and zinc phosphates and pyromorphite when different concentrations of oxalic acid were used allowed us to estimate which approximate total oxalate concentrations could cause the solubilization haloes formed by *B. caledonica* in the agar microcosms (data not shown). It seemed that fungal solubilization of cadmium phosphate and pyromorphite could be equivalent to the excretion of nearly 50 μmol of oxalic acid into the agar by *B. caledonica* and that for zinc and copper phosphate solubilization the values could be even higher.

Overexcretion of oxalic acid by the fungus led to the transformation of all metal minerals into metal oxalates (Fig. 4 and 5). *B. caledonica* turned cadmium phosphate into tabular crystals of cadmium oxalate (Fig. 4A and 5A); all copper-containing minerals tested into twinned fourling crystals of copper oxalate hydrate (moolooite) (Fig. 4B and 5B); zinc phosphate into twinned bulbous crystals of zinc oxalate dihydrate (Fig. 4C and 5C); and all lead compounds tested into single prismatic crystals of lead oxalate and dendritic aggregates of crystals (Fig. 4D and E and 5D).

During growth of *B. caledonica* in the presence of copper phosphate or cuprite, it was often observed that moolooite crystals precipitated in the bottom of the petri dish, forming concentric ring patterns (data not shown). These patterns were very similar to Liesegang patterns, which are formed by a complex interplay of diffusion, chemical reaction, and precipitation during reaction-diffusion processes (26). The mechanism of Liesegang ring formation is based on prenucleation supersaturation of the medium; nucleating particles deplete their surroundings of product, which causes a drop in the local level of supersaturation such that the nucleation rate in the neighborhood decreases, leading to spacing between regions of nucleation that gives rise to rings (26). For Liesegang phenomena, the ratio of the width of the nth ring to the distance between the center of the system and the nth ring is constant, and calculations of this ratio for moolooite precipitates gave a constant value, which confirmed the reaction-diffusion nature of the process mediated by the fungus in our system.

For cadmium-, copper-, and zinc-containing minerals, precipitation of metal oxalates was observed not only in the agar but also on the fungal mycelium above the dialysis membrane (Fig. 2D and 6). Oxalate crystals could be entrapped in fungal hyphae (Fig. 6C), and when grown on copper phosphate, the mycelial cords formed by *B. caledonica* were encrusted with moolooite crystals (Fig. 2D and 6A). Scanning electron microscopy (wet-mode ESEM) revealed that crystals were embedded in the well-hydrated mucilaginous sheath that covered the fungal biomass (Fig. 6B and D) and that crystals overprecipitated around fungal hyphae, leaving a net of fungal tunnels within the mineral phase (as determined by cryo-SEM with cryofracturing) (Fig. 6E and F).

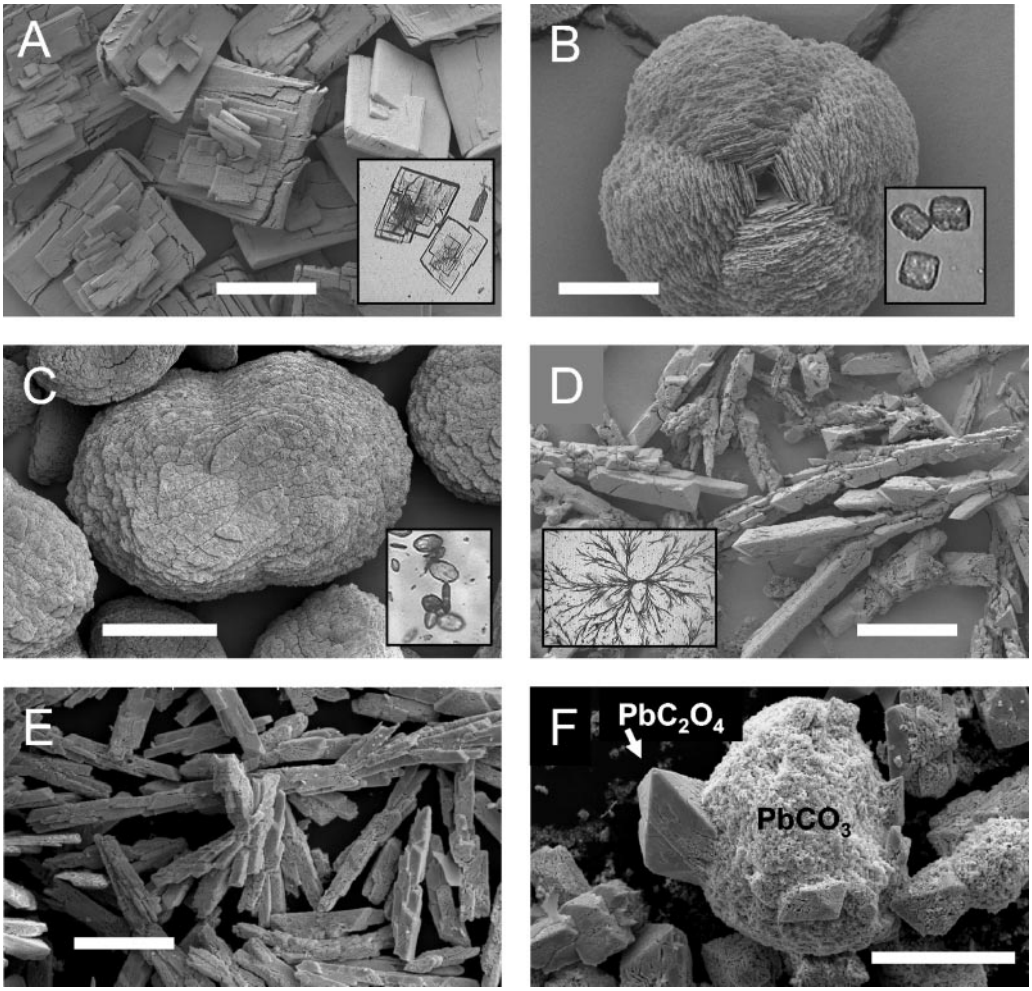

FIG. 4. SEM images of air-dried Au-Pd-coated metal oxalate crystals extracted from the agar media after growth of *B. caledonica* on toxic metal minerals. (A) Cadmium oxalate formed in the presence of cadmium phosphate; (B) copper oxalate hydrate (moolooite) formed in the presence of copper phosphate; (C) zinc oxalate dihydrate formed in the presence of zinc phosphate; (D to F) lead oxalate formed in the presence of lead phosphate (D), lead tetraoxide (E), and lead carbonate (F). The insets in panels A to D are light microscopic images of the same metal oxalates in the agar before extraction. (A) Scale bar = 500 μm; (B) scale bar = 15 μm; (C to F) scale bars = 100 μm.

Metals mobilized by *B. caledonica* were accumulated not only within extracellular crystalline oxalate precipitates but also within the fungal biomass. Analysis of crystal-free mycelium grown on agar containing zinc phosphate and pyromorphite showed that hyphae accumulated zinc and lead at levels around 3 and 6 mg g (dry weight) of biomass^{-1}, respectively. When the organism was grown on copper phosphate-containing medium, the level of copper that was accumulated by the moolooite-precipitating mycelium was approximately 100 mg g (dry weight)$^{-1}$, which was more than 10 times the values for zinc and lead. Well-structured moolooite crystals precipitated on the mycelium comprised approximately 35% of the total copper accumulated by the mycelium.

The EXAFS spectrum and Fourier transform of fungal biomass grown on copper phosphate with numerous moolooite crystals were very similar to those of the copper oxalate hydrate standard, which confirmed that copper was coordinated by carboxylic ligands in the mycelium (Fig. 7A to C; Cu K-edge EXAFS parameters are not shown). There were three clear peaks in the Fourier transform, and the spectrum could be fitted with effectively the same parameters. In the copper oxalate hydrate standard, the outer shells were slightly better defined, which may have been an effect of grain size in the sample or a slight degree of noncrystallinity, suggesting that there were amorphous carboxylic complexes of copper within the mycelium.

The EXAFS spectra and Fourier transforms of fungal biomass grown on both pyromorphite- and lead tetraoxide-containing media could be fitted with two shells of oxygen scatterers at slightly different distances, reflecting lead coordination by oxygen ligands [Fig. 7D to F; Pb L(III)-edge EXAFS parameters are not shown]. There was improvement in the fit of pyromorphite-grown biomass after addition of a further shell of phosphorus scatterers, implying that there was phosphate coordination within the mycelium.

DISCUSSION

The present study was the first study in which the mineral-solubilizing and -transforming abilities of *B. caledonica*, a representative of the entomopathogenic group of fungi, were eval-

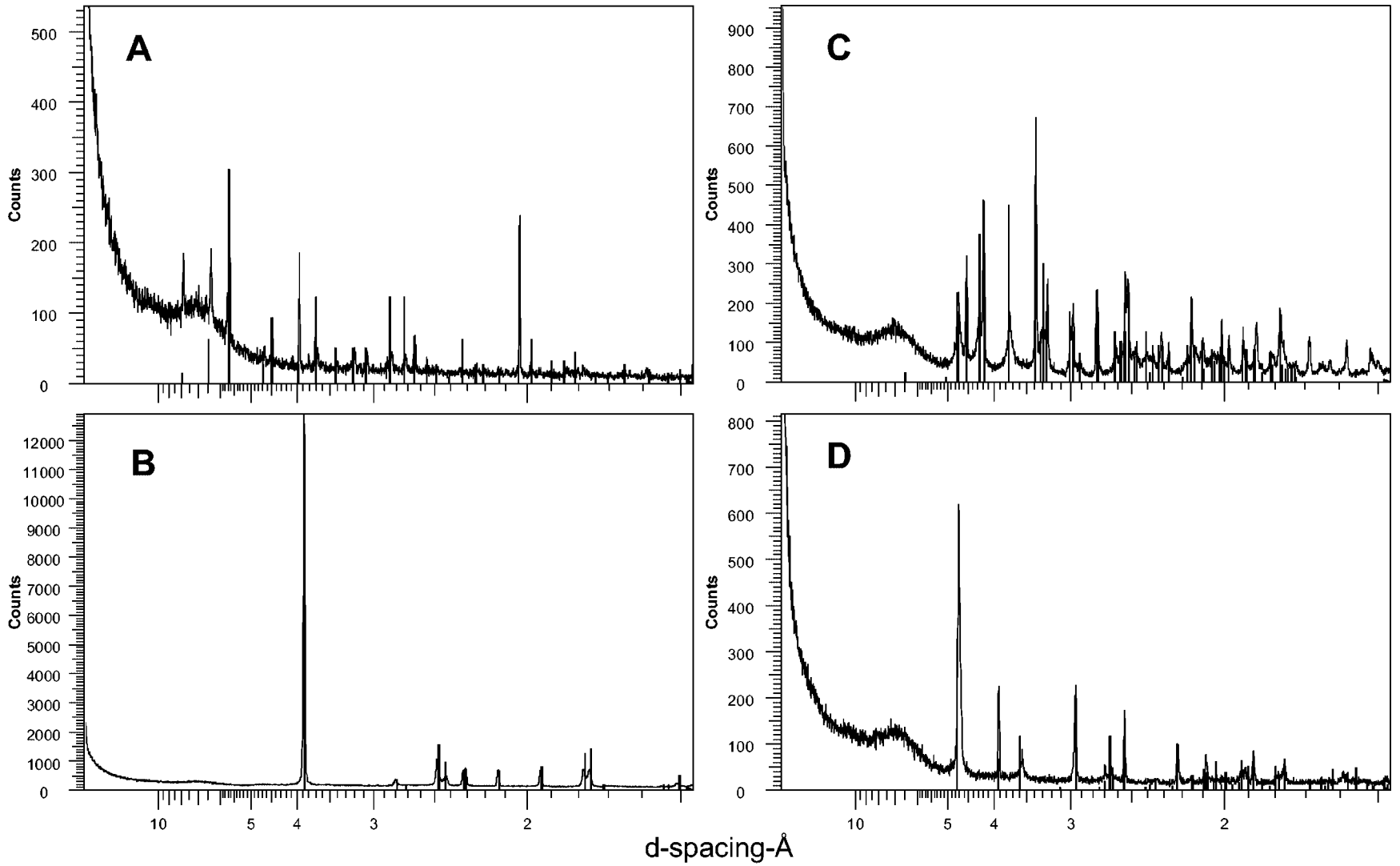

FIG. 5. Typical XRPD patterns for metal oxalate crystals precipitated by *B. caledonica* in agar media or in the mycelium. (A) Cadmium oxalate formed on medium containing cadmium phosphate; (B) copper oxalate hydrate (moolooite) formed on medium containing copper phosphate or cuprite; (C) lead oxalate formed on medium containing lead phosphate, lead tetraoxide, lead sulfide, lead carbonate, and pyromorphite; (D) zinc oxalate dihydrate formed on medium containing zinc phosphate. The vertical bars indicate the peak positions and relative intensities for standard XRPD patterns of metal oxalates as given in the International Centre for Diffraction Data powder diffraction file. The standards used were cadmium oxalate (PDF-14-0712), copper oxalate hydrate (PDF-21-0297), lead oxalate (PDF-14-0803), and zinc oxalate dihydrate (PDF-25-1029). Typical spectra are shown from one of several plots.

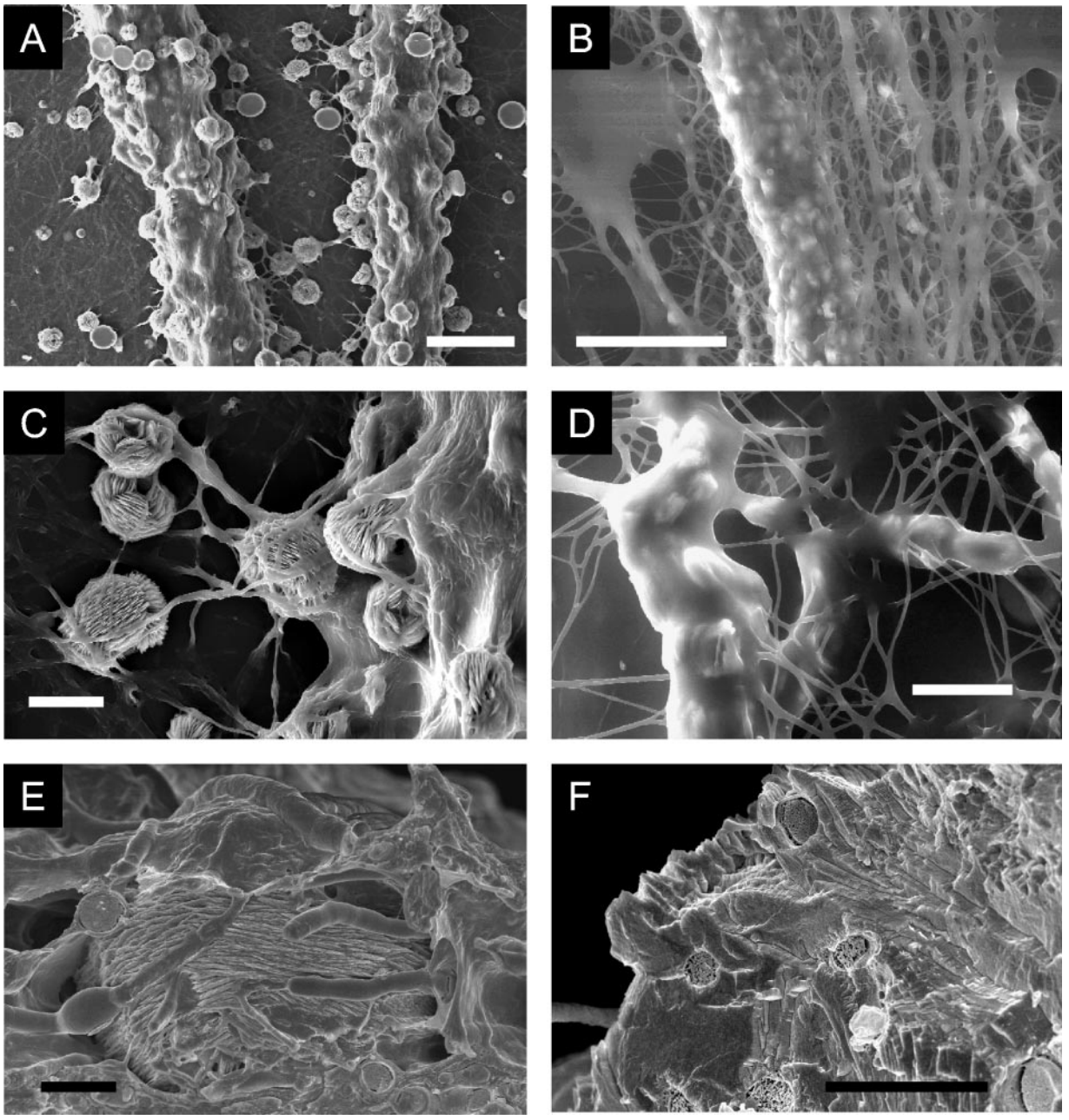

FIG. 6. SEM images of moolooite precipitation by *B. caledonica* hyphae and cords when the organism was grown on agar medium containing copper phosphate. (A and C) High-vacuum-mode ESEM images of air-dried Au-Pd-coated samples; (B and D) wet-mode ESEM images of hydrated samples, revealing a thick mucilaginous sheath covering the mycelium and crystals; (E and F) cryo-SEM images of cryopreserved and cryofractured samples providing experimental evidence of the presence of the parental fungal hyphae within a mycogenic mineral. (A) Scale bar = 100 μm; (B) scale bar = 50 μm; (C and D) scale bars = 20 μm; (E and F) scale bars = 5 μm.

uated. This organism was able to solubilize and transform a wide range of cadmium-, copper-, zinc-, and lead-containing insoluble minerals. Only one example of fungal dissolution of a lead-containing mineral (pyromorphite) has been described for *Aspergillus niger* (44). Amazingly, *B. caledonica* dissolved and transformed into lead oxalates all lead-containing minerals tested (pyromorphite and lead phosphate, carbonate, sulfide, and tetraoxide). It seems likely that the major mechanism of mineral dissolution was ligand promoted. The fungus excreted substantial concentrations of acetic, citric, and oxalic acids during growth in the presence of toxic metal minerals. The nature and amount of organic acids excreted by fungi are mainly influenced by the pH and buffering capacity of the environment, the carbon, phosphorus, and nitrogen sources, and the presence of certain metals (8, 13, 19, 30, 31, 32). Toxic metals may increase oxalate excretion by fungi; e.g., the presence of copper uniformly stimulated organic acid production by brown rot basidiomycetes (10). The presence of zinc phos-

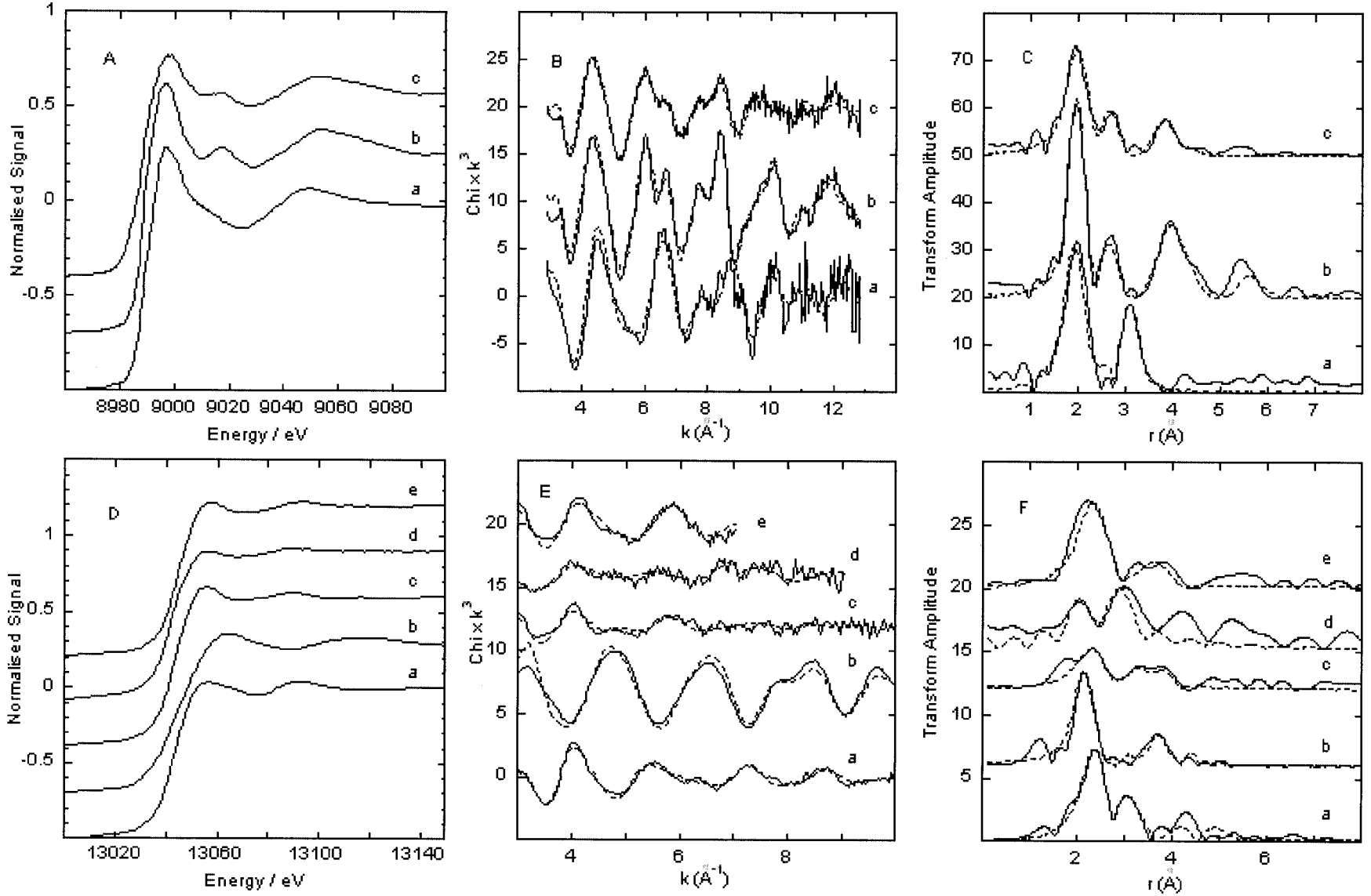

FIG. 7. (A) Cu K-edge X-ray absorption near-edge structure (XANES) spectra of a copper phosphate standard (line a), a moolooite standard (line b), and *B. caledonica* biomass grown on medium containing copper phosphate (line c); (B) corresponding EXAFS spectra (solid lines) and fits (dotted lines) of the three samples; (C) Fourier transforms of the spectra and fits. (D) Pb L(III)-edge XANES spectra of a lead oxalate standard (line a), a lead tetraoxide standard (line b), a pyromorphite standard (line c), *B. caledonica* biomass grown on medium containing lead tetraoxide (line d), and *B. caledonica* biomass grown on medium containing pyromorphite (line e); (E) corresponding EXAFS spectra (solid lines) and fits (dotted lines) of the five samples; (F) Fourier transforms of the spectra and fits. The amplitude of the lead tetraoxide Fourier transforms was reduced for ease of comparison.

phate in the medium markedly influenced citric acid production by *A. niger* (45). In the present study, cuprite and zinc phosphate caused a dramatic increase in citric acid synthesis. An examination of the dynamics of organic acid synthesis and the amounts of the organic acids showed that the overexcretion of oxalate played the main role in mineral solubilization and transformation processes. Oxalic acid is a well-known chelating agent that has been widely studied because of its ability to dissolve different minerals, from natural rocks to dental cement (4, 29, 38, 40, 45, 53). In contrast to other low-molecular-weight carboxylic acids with low complexing abilities that erode minerals in acid solution by protonolysis (e.g., acetic and lactic acids), oxalic acid is able to mobilize metals very efficiently at neutral pH and even in basic solutions (38).

Fungi such as phytopathogens and wood rotters are often reported to overexcrete oxalic acid (9, 13, 20, 35, 41). It has been suggested that oxalic acid is involved in nonenzymatic initiation of wood cell wall depolymerization through the production of free radical species in the early stages of both lignin and cellulose degradation by wood-rotting fungi (20, 35). Plant pathogens can generate and secrete into their surroundings millimolar concentrations of oxalate (9, 41), and such oxalic acid production during plant infection has been implicated as a primary determinant of pathogenicity (13). One of the main functions of oxalate secretion by *Sclerotinia* during plant pathogenesis is the suppression of active oxygen generation, which compromises the defense responses of the host (9). *Beauveria* germ tubes penetrate the leaf cuticle in an endophytic relationship just as they penetrate the cuticle of insects during entomopathogenesis (48). Oxalate overexcretion by *Beauveria* probably plays a role in facilitating the penetration processes similar to the role that oxalate overexcretion plays in phytopathogenic and/or wood-rotting fungi.

Solubilization of cadmium-, copper-, zinc-, and lead-containing minerals increases toxic metal mobility and therefore the apparent bioavailability of the minerals to the fungus. However, *B. caledonica* was extremely metal tolerant. One aspect of toxic metal tolerance, which was easily observed even with the naked eye, was a change in mycelial growth. Mycelial aggregation represented by the phalanx (or slow dense) strategy is well known for its protective function and has been observed for fungi colonizing toxic metal-contaminated domains (16). In the present study, depending on the nature of the insoluble mineral, *B. caledonica* adopted the phalanx (slow dense) strategy and even the cord-forming (reallocation) strategy (17), with the result that it tolerated the toxic metal stress but maintained a high biomass yield. Other mechanisms of fungal defense against metal toxicity are chemical, biochemical, and physiological, including extracellular metal sequestration and precipitation, metal binding to the walls, intracellular sequestration and complexation, and compartmentation or volatilization (18). As revealed by X-ray absorption spectroscopy, both copper and lead within the *B. caledonica* mycelium were coordinated by oxygen ligands. Copper was coordinated by carboxylic groups, a considerable proportion of which were derived from oxalate and were either crystalline or amorphous. Lead, which was mobilized from pyromorphite, was coordinated by phosphate groups within the biomass. It is known that polyphosphate granules, which are localized in fungal vacuoles, may be important in intracellular homeostasis and can incorporate metal cations, including those of potentially toxic metals (6). It could be suggested that an excess of mobile lead was sequestered by an excess of phosphorus species mobilized after pyromorphite dissolution, perhaps resulting in some secondary lead phosphate formation but with some lead possibly located within polyphosphates.

Metal toxicity may be reduced if the mobilized toxic metal forms complexes with organic ligands excreted by the fungus and especially if toxic metals are precipitated as highly insoluble oxalates (18). The induction of oxalic acid efflux correlated closely with copper tolerance in brown rot fungi (21), and overexcretion of oxalic acid probably contributed to the metal tolerance exhibited by *B. caledonica* in the present study.

The existence of mucilaginous sheaths around hyphae has been reported for a wide range of fungi, and the functions of these sheaths include protection and attachment. In our study, the sheath provided a matrix for fungus-mineral interactions and metal transformations, harboring mineral-weathering and metal-chelating agents and resulting in crystal growth and deposition of secondary mycogenic minerals, such as calcium and copper oxalates, and, with sorption phenomena, presumably affected the diffusion of mobile metal species (12, 14, 24, 28, 47, 50). In our wet-mode ESEM study, all the processes of metal diffusion and precipitation of metal oxalates occurred in this well-hydrated mucilaginous microenvironment, which was impossible to observe by conventional SEM in high-vacuum mode. Moreover, the overexudation of oxalate by *B. caledonica* led to so much crystal growth within the fungal colony that newly formed mycogenic crystalline aggregates covered the parental hyphal net. Using cryo-SEM, we demonstrated for the first time a new aspect of the interactions between fungal and mineral matter, i.e., the presence of hyphae within mycogenic minerals. This finding may highlight a role for oxalate-overexcreting fungi in the evolution of certain minerals.

In biotechnological terms, it is possible that entomopathogenic fungi could be used for commercial applications other than just pest control. The unique mineral-transforming ability and toxic metal tolerance of *B. caledonica* could have applications in some bioremediation and bioleaching processes. The potential of *B. caledonica* for overproduction of oxalic acid in amounts comparable to the amounts produced by *A. niger* under controlled conditions (46) could have some benefits for biological production of oxalic acid. It may be time to pay attention to the much wider and complex ecological and biotechnological significance of this group of fungi.

ACKNOWLEDGMENTS

This research was funded by the BBSRC/BIRE program (grant 94/BRE13640), BNFL, and CLRC Daresbury Synchrotron Radiation Source (Synchrotron Radiation Source user grant 40107).

We thank David Genney (University of Aberdeen, Aberdeen, Scotland) for providing the fungal strain. We are very grateful to Lorrie Murphy and Bob Bilsborrow (stations 7.1 and 16.5, CLRC Daresbury Synchrotron Radiation Source, Daresbury, United Kingdom) for their help with X-ray absorption spectroscopy and to Martin Kierans (Centre for High Resolution Imaging and Processing, School of Life Sciences, University of Dundee, Dundee, Scotland) for assistance with scanning electron microscopy.

REFERENCES

1. **Binsted, N.** 1998. Daresbury Laboratory EXCURV98 program. Daresbury Laboratory, Daresbury, Warrington, Cheshire, United Kingdom.

2. **Binsted, N., R. W. Strange, and S. S. Hasnain.** 1992. Constrained and restrained refinement in EXAFS data analysis with curved wave theory. Biochemistry **31:**12117–12125.
3. **Bisset, J., and P. Widden.** 1986. A new species of *Beauveria* isolated from Scottish moorland soil. Can. J. Bot. **66:**361–362.
4. **Borggaard, O. K.** 1992. Dissolution of poorly crystalline iron oxides by EDTA and oxalate. Z. Pflanzenernaehr Bodenkd. **155:**431–436.
5. **Bruck, D. J., and L. C. Lewis.** 2002. Rainfall and crop residue effects on soil dispersion and *Beauveria bassiana* spread to corn. Appl. Soil Ecol. **20:**183–190.
6. **Bucking, H., and W. Heyser.** 1999. Elemental composition and function of polyphosphates in ectomycorrhizal fungi—an X-ray microanalytical study. Mycol. Res. **103:**31–39.
7. **Burford, E. P., M. Fomina, and G. M. Gadd.** 2003. Fungal involvement in bioweathering and biotransformation of rocks and minerals. Miner. Mag. **67:**1127–1155.
8. **Burgstaller, W., and F. Schinner.** 1993. Leaching of metals with fungi. J. Biotechnol. **27:**91–116.
9. **Cessna, S. G., V. E. Sears, M. B. Dickman, and P. S. Low.** 2000. Oxalic acid, a pathogenicity factor for *Sclerotinia sclerotiorum*, suppresses the oxidative burst of the host plant. Plant Cell **12:**2191–2200.
10. **Clausen, C. A., and F. Green.** 2003. Oxalic acid overproduction by copper-tolerant brown-rot basidiomycetes on southern yellow pine treated with copper-based preservatives. Int. Biodeterior. Biodegrad. **51:**139–144.
11. **Colpaert, J. V., P. Vandenkoornhuyse, K. Adriaensen, and J. Vangronsveld.** 2000. Genetic variation and heavy metal tolerance in the ectomycorrhizal basidiomycete *Suillus luteus.* New Phytol. **147:**367–379.
12. **Connolly, J. H., and J. Jellison.** 1995. Calcium translocation, calcium oxalate accumulation, and hyphal sheath morphology in the white rot fungus *Resinicium bicolor*. Can. J. Bot. **73:**927–936.
13. **Dutton, M. V., and C. S. Evans.** 1996. Oxalate production by fungi: its role in pathogenicity and ecology in the soil environment. Can. J. Microbiol. **42:**881–895.
14. **Elinov, N. P., E. P. Anan'eva, and G. A. Yaskovich.** 1999. Activity of exoglycans as sorbents of ions of heavy metals. Appl. Biochem. Microbiol. **35:**168–171.
15. **Elliot, S. L., M. W. Sabelis, A. Janssen, L. P. S. van der Geest, E. A. M. Beerling, and J. Fransen.** 2000. Can plants use entomopathogens as bodyguards? Ecol. Lett. **3:**228–235.
16. **Fomina, M., K. Ritz, and G. M. Gadd.** 2003. Nutritional influence on the ability of fungal mycelia to penetrate toxic metal-containing domains. Mycol. Res. **107:**861–871.
17. **Fomina, M., E. P. Burford, and G. M. Gadd.** Toxic metals and fungal communities. *In* J. Dighton, J. White, and P. Oudemans (ed.), The fungal community: its organization and role in the ecosystem, in press. CRC Press, Boca Raton, Fla.
18. **Gadd, G. M.** 1993. Interactions of fungi with toxic metals. New Phytol. **124:**25–60.
19. **Gadd, G. M.** 1999. Fungal production of citric and oxalic acid: importance in metal speciation, physiology and biogeochemical processes. Adv. Microb. Physiol. **41:**48–92.
20. **Goodell, B.** 2003. Brown-rot fungal degradation of wood: our evolving view. Wood Deterior. Preserv. **845:**97–118.
21. **Green, F., and C. A. Clausen.** 2003. Copper tolerance of brown-rot fungi: time course of oxalic acid production. Int. Biodeterior. Biodegrad. **51:**145–149.
22. **Gurman, S. J., N. Binsted, and I. Ross.** 1984. A rapid, exact, curved-wave theory for EXAFS calculations. J. Phys. C **17:**143–151.
23. **Gurman, S. J., N. Binsted, and I. Ross.** 1986. A rapid, exact, curved-wave theory for EXAFS calculations. 2. The multiple-scattering contributions. J. Phys. C **19:**1845–1861.
24. **Gutierrez, A., M. J. Martinez, G. Almendros, F. J. Gonzalezvila, and A. T. Martinez.** 1995. Hyphal-sheath polysaccharides in fungal deterioration. Sci. Total Environ. **167:**315–328.
25. **Hedin, L., and S. Lundqvist.** 1969. Effects of electron-electron and electron-phonon interactions on the one-electron states of solids. Solid State Phys. **23:**1–181.
26. **Henisch, H. K.** 2002. Crystals in gels and Liesegang rings, p. 212. Cambridge University Press, Cambridge, United Kingdom.
27. **Hughes, K. A., and B. Lawley.** 2003. A novel Antarctic microbial endolithic community within gypsum crusts. Environ. Microbiol. **5:**555–557.
28. **Jellison, J., Y. Chen, and F. A. Fekete.** 1997. Hyphal sheath and iron-binding compound formation in liquid cultures of wood decay fungi *Gloeophyllum trabeum* and *Postia placenta.* Holzforschung **51:**503–510.
29. **Klarup, D.** 1997. The influence of oxalic acid on release rates of metals from contaminated river sediment. Sci. Total Environ. **204:**223–231.
30. **Kubicek, C. P.** 1998. Citric acid production, p. 236–257. *In* T. Nagodawithana and G. Reed (ed.), Commercial fermentations and nutritional needs of their microorganisms. Esteekay Associates Inc., Milwaukee, Wis.
31. **Kubicek, C. P., and M. Roehr.** 1986. Citric acid fermentation. Crit. Rev. Biotechnol. **3:**331–373.
32. **Lapeyrie, F., G. A. Chilvers, and C. A. Bhem.** 1987. Oxalic acid synthesis by the mycorrhizal fungus *Paxillus involutus* (Batsch, ex Fr.). New Phytol. **106:**139–146.
33. **Lapeyrie, F., J. Ranger, and D. Vairelles.** 1991. Phosphate-solubilizing activity of ectomycorrhizal fungi *in vitro.* Can. J. Bot. **69:**342–346.
34. **Leyval, C., and E. J. Joner.** 2001. Bioavailability of heavy metals in the mycorrhizosphere, p. 165–185. *In* G. R. Gobran, W. W. Wenzel, and E. Lombi (ed.), Trace elements in the rhizosphere. CRC Press, Boca Raton, Fla.
35. **Machuca, A., D. Napoleao, and A. M. F. Milagres.** 2001. Detection of metal-chelating compounds from wood-rotting fungi *Trametes versicolor* and *Wolfiporia cocos.* World J. Microbiol. Biotechnol. **17:**687–690.
36. **Manley, E., and L. Evans.** 1986. Dissolution of feldspars by low-molecular-weight aliphatic and aromatic acids. Soil Sci. **141:**106–112.
37. **Martino, E., S. Perotto, R. Parsons, and G. M. Gadd.** 2003. Solubilization of insoluble inorganic zinc compounds by ericoid mycorrhizal fungi derived from heavy metal polluted sites. Soil Biol. Biochem. **35:**133–141.
38. **Matsuya, S., and Y. Matsuya.** 1994. Dissolution of dental zinc phosphate cement in organic acid solution. J. Ceramic Soc. Jpn. **102:**414–418.
39. **Muller, B., W. Burgstaller, H. Strasser, A. Zanella, and F. Schinner.** 1995. Leaching of zinc from an industrial filter dust with *Penicillium*, *Pseudomonas* and *Corynebacterium*: citric acid is the leaching agent rather than amino acids. J. Ind. Microbiol. **14:**208–212.
40. **Panias, D., M. Taxiarchou, and A. Kontopoulos.** 1996. Mechanisms of dissolution of iron oxides in aqueous oxalic acid solutions. Hydrometallurgy **42:**257–265.
41. **Rollings, J. A., and M. B. Dickman.** 2001. pH signaling in *Sclerotinia sclerotiorum*: identification of a pacC/RIM1 homolog. Appl. Environ. Microbiol. **67:**75–81.
42. **Sayer, J. A., S. L. Raggett, and G. M. Gadd.** 1995. Solubilization of insoluble compounds by soil fungi: development of a screening method for solubilizing ability and metal tolerance. Mycol. Res. **99:**987–993.
43. **Sayer, J. A., and G. M. Gadd.** 1997. Solubilisation and transformation of insoluble metal compounds to insoluble metal oxalates by *Aspergillus niger.* Mycol. Res. **101:**653–661.
44. **Sayer, J. A., J. D. Cotter-Howells, C. Watson, S. Hillier, and G. M. Gadd.** 1999. Lead mineral transformation by fungi. Curr. Biol. **9:**691–694.
45. **Sayer, J. A., and G. M. Gadd.** 2001. Binding of cobalt and zinc by organic acids and culture filtrates of *Aspergillus niger* grown in the absence or presence of insoluble cobalt or zinc phosphate. Mycol. Res. **105:**1261–1267.
46. **Strasser, H., W. Burgstaller, and F. Schinner.** 1994. High yield production of oxalic acid for metal leaching purposes by *Aspergillus niger.* FEMS Microbiol. Lett. **119:**365–370.
47. **Sutter, H. P., E. B. G. Jones, and O. Walchi.** 1984. Occurrence of crystalline hyphal sheaths in *Poria placenta* (Fr.) Cke. J. Inst. Wood Sci. **10:**19–23.
48. **Wagner, B. L., and L. C. Lewis.** 2000. Colonization of corn, *Zea mays*, by the entopathogenic fungus *Beauveria bassiana.* Appl. Environ. Microbiol. **66:**3468–3473.
49. **Wallander, H., T. Wickman, and G. Jacks.** 1997. Apatite as a source in mycorrhizal and non-mycorrhizal *Pinus sylvestris* seedlings. Plant Soil **196:**123–131.
50. **Welch, S. A., W. W. Barker, and J. F. Banfield.** 1999. Microbial extracellular polysaccharides and plagioclase dissolution. Geochim. Cosmochim. Acta **63:**1405–1419.
51. **White, J. F., F. Belanger, W. M. Meyer, R. F. Sullivan, J. F. Bischoff, and E. A. Lewis.** 2002. Clavicipitalean fungal epibionts and endophytes—development of symbiotic interactions with plants. Symbiosis **33:**201–213.
52. **White, T. J., T. D. Bruns, S. Lee, and J. Taylor.** 1990. Analysis of phylogenetic relationships by amplification and direct sequencing of ribosomal RNA genes, p. 315–322. *In* M. A. Innis, D. H. Gelfand, J. J. Sninsky, and T. J. White (ed.), PCR protocols: a guide to methods and applications. Academic Press, New York, N.Y.
53. **Xyla, A. G., B. Sulzberger, G. W. Lither III, J. G. Hering, P. van Cappellen, and W. Stumm,.** 1992. Reductive dissolution of manganese(III, IV) (hydr)-oxides by oxalate: the effect of pH and light. Langmuir **8:**95–103.